Hyperfine structure of the $4f^7 5d^2 6s\ ^{11}F$ term of ^{155,157}Gd I by laser-rf double resonance

W. J. Childs
Physics Division, Argonne National Laboratory, Argonne, Illinois 60439
(Received 19 December 1988)

The atomic-beam laser-rf double-resonance method has been used to measure the hyperfine structure (hfs) of the $J=2$–8 levels of the ^{11}F term of $4f^7 5d^2 6s$ in ^{155,157}Gd I. Results are also reported for the $J=2,5$ levels of the ^7D term of $4f^7 5d 6s^2$. Less precise hfs results are given for ten highly excited even-parity levels, and isotope shifts are given for 16 optical lines. L-S limit effective-operator expressions are given for the hfs A and B values of arbitrary states built from three open electron shells. When specialized to the ^{11}F term in Gd I, these expressions reveal a marked perturbation between the $J=5$ levels of $4f^7 5d^2 6s\ ^{11}F$ and $4f^7 5d 6s^2\ ^7D$. The perturbation can also be detected from the fine-structure intervals.

I. INTRODUCTION

The neutral gadolinium atom lies near the middle of the $4f$ shell, and its electronic states are consequently very complex. A great deal of spectroscopic work has been done, however, and a large number of levels have been identified through the systematic study of thousands of lines.[1] Most of the low-lying odd-parity levels (and some of the even ones) have a half-filled $4f$ shell coupled to ^8S plus three other valence electrons. Although this feature may somewhat simplify the spectroscopic situation, the $4f^7$ core still creates an extremely difficult problem for *ab initio* calculations.

Over the years many investigations of hyperfine structure (hfs) have been carried out in the rare-earth ($4f$-shell) region,[2] partly because of the challenge of such complex systems. Most of the attention has been focused on the simplest $4f$ configurations, $4f^N 6s^2$, that appear in several of the neutral lanthanide atoms.[3] The only precise study of hfs in the odd-A Gd isotopes ^{155,157}Gd so far is that of Unsworth *et al.* in 1969, who measured[4] the hfs of the ground ^9D term in the $4f^7 5d 6s^2$ configuration. They found that the amount of contact hfs is very small and that the radial integral associated with the spin-dipole hfs interaction is only about half has large as that for the orbital part. One especially interesting finding was that because of the large size of the nuclear electric quadrupole moments in ^{155,157}Gd, the quadrupole hfs is often comparable to the dipole.

The goal of the present work was to extend the earlier studies to the other two low-lying configurations $4f^7 5d^2 6s$ and $4f^8 6s^2$. The first of these goals is achieved, but the second will require much greater sensitivity than that available to us. Although this sort of multiconfiguration information will eventually have to be understood in terms of the *ab initio* theory, we can at present only try to understand it with the semiempirical effective-operator approach. This is shown to be extremely successful in accounting for the measured hfs, however, even for that arising from three open electron shells. Such hfs studies are also a requirement for extracting isotope shifts involving the odd-A isotopes. This is an area of continuing interest[5,6] independent of the hfs itself.

II. EXPERIMENT

The present measurements were carried out using (a) laser-excited fluorescence and (b) laser-radio-frequency double resonance, both in a thermal atomic beam of gadolinium. Since the laser beam and the atomic beam were orthogonal, the fluorescence spectra were Doppler free to first order. The linewidth of about 20 MHz arose primarily from imperfect collimation of the atomic beam. For the double-resonance measurements, the laser beam was split into two parts: a strong "pump" beam which intersected the atomic beam near its source, and the weaker "probe" beam (mentioned above) which produced fluorescence about 40 cm further downstream. When the laser was tuned to a particular hyperfine component of an optical line, the pump beam strongly depleted the population of the lower hfs level of the component. The probe beam was then unable to induce much fluorescence unless the depleted level was repopulated in the space between the pump and probe regions. This was done by driving a rf transition between a filled hfs level and the depleted level, causing a strong resonant increase in the fluorescence induced downstream by the probe beam. The linewidth [full width at half maximum (FWHM)] observed for such rf transitions was determined by the transit time of the atoms through the radio-frequency field and was typically 10 kHz.

The apparatus has been described previously;[7] no significant changes were required. The Gd beam was produced by electron-bombardment heating of a Ta crucible (2-cm tall by 0.7-cm diam). The beam was formed by gadolinium atoms effusing through a 1-mm hole in the top. Substantial population of high-lying metastable levels was achieved by maintaining a discharge in the atomic beam at the oven exit hole. The laser was a Coherent Radiation 699-21 cw ring dye laser driven by an argon-ion laser. A Hall-Lee-type[8] wave meter was used to measure

the laser wavelength, and incremental frequency markers spaced 150 MHz apart were obtained for calibrating laser sweeps by passing some of the laser light through a Burleigh 50-cm confocal Fabry-Pérot étalon. The fluorescence produced by the probe beam was collected by an ellipsoidal reflector and detected by a cooled photon-counting photomultiplier (PM). For most of the lines studied, the fluorescence was detected well to the blue of the exciting laser wavelength. Interference filters (FWHM of 100 Å) were placed in front of the PM tube to exclude scattered laser photons and to reduce background light from the very hot atomic-beam oven. The radio frequencies were generated by a 0–1-GHz frequency synthesizer.

Table I summarizes the known information about the upper and lower levels of all the lines studied and gives the central wavelength of the (bandpass) interference filter used for detection. All of the lines in the table have been tabulated by Meggers *et al.*[9] except those at 5868.90, 5872.64, 5916.73, 5923.26, and 5997.98 Å. The wavelengths listed are those measured with the wave meter.

Figure 1 shows a laser scan through the region of the known line at 5916.75 Å between the $^{11}F_5$ state of $4f^7 5d^2 6s$ at 7103 cm^{-1} and an excited $J=5$ level at 23 999 cm^{-1}. Study of the hfs components showed that the scan contains a second line (at 5916.73 Å) connecting the $^7D_2$ level of $4f^7 5d 6s^2$ at 7562 cm^{-1} with an excited $^7P_2$ level at 24 458 cm^{-1}. Both lines are listed in Table I. Figure 1 was obtained using a 4200-Å interference filter; it was found that a 4400-Å filter eliminates only the 5916.73-Å line, while a 4100-Å filter eliminates only the line at 5916.75 Å. The numbers in large type on Fig. 1 identify components due to even-A Gd isotopes in 5916.75, while the smaller numbers identify the same components for the line at 5916.73 Å. It is immediately seen that the isotope shifts for the two lines are very different.

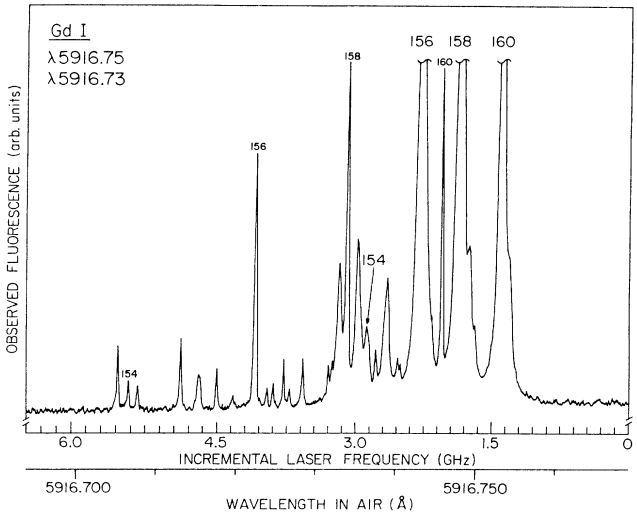

FIG. 1. Fluorescence observed through a 4200-Å interference filter as the laser is scanned around the wavelength 5916.7 Å. The hfs components in the fluorescence pattern arise from two distinct excitation lines as described in the text and Table I. The two lines have very different isotope shifts.

The procedure for measuring the hfs for a line was to sweep the laser several times through the line, recording both the fluorescence intensity and the frequency markers mentioned above. The observed structure of each line arises from the contributions of the seven stable Gd isotopes. Because of the very large nuclear electric quadru-

TABLE I. Optical lines studied. Columns 2–4 and 5–7 give the known information about the lower and upper states, respectively, and the final column gives the central wavelength of the bandpass interference filter used to detect the upper-state fluorescence. The excitation energies are from Ref. 1, and the observed wavelengths are the present measurements.

Observed λ (air) (Å)	Lower level			Upper level			Filter used (Å)
	Electron configuration	Nominal S,L,J	Excitation energy (cm^{-1})	Electron configuration	Nominal S,L,J	Excitation energy (cm^{-1})	
5633.48	$4f^7 5d^2 6s$	$^{11}F_5^0$	7103.420	$4f^7 5d 6s 6p$	$J=4$	24 849.514	4200
5692.10	$4f^7 5d^2 6s$	$^{11}F_6^0$	7480.348	$4f^7 5d 6s 6p$	$J=5$	25 043.649	4200
5735.96	$4f^7 5d^2 6s$	$^{11}F_7^0$	7947.294	$4f^7 5d 6s 6p$	$J=7$	25 376.313	4200
5754.14	$4f^7 5d^2 6s$	$^{11}F_6^0$	7480.348	$4f^8 5d 6s$	$^9G_6$	24 854.297	4200
5807.70	$4f^7 5d^2 6s$	$^{11}F_4^0$	6786.184	$4f^7 5d 6s 6p$	$J=5$	23 999.912	4200
5868.90	$4f^8 6s^2$	$^7F_6$	10 947.210	$4f^8 6s 6p$	$J=7$	27 981.472	5900
5872.64	$4f^7 5d 6s^2$	$^7D_5^0$	6976.508	$4f^7 5d 6s 6p$	$J=5$	23 999.912	4200
5916.73	$4f^7 5d 6s^2$	$^7D_2^0$	7562.457	$4f^7 5d 6s 6p$	$^7P_2$	24 458.988	4100
5916.75	$4f^7 5d^2 6s$	$^{11}F_5^0$	7103.420	$4f^7 5d 6s 6p$	$J=5$	23 999.912	4200
5923.26	$4f^7 5d^2 6s$	$^{11}F_8^0$	8498.434	$4f^7 5d 6s 6p$	$J=7$	25 376.313	4200
5930.27	$4f^7 5d^2 6s$	$^{11}F_4^0$	6786.184	$4f^7 5d 6s 6p$	$J=4$	23 644.156	4200
5936.80	$4f^7 5d^2 6s$	$^{11}F_3^0$	6550.395	$4f^7 5d 6s 6p$	$J=3$	23 389.782	4200
5937.70	$4f^7 5d^2 6s$	$^{11}F_2^0$	6378.146	$4f^7 5d 6s 6p$	$J=2$	23 215.028	4200
5977.23	$4f^7 5d^2 6s$	$^{11}F_2^0$	6378.146	$4f^7 5d^2 6p$	$J=1$	23 103.660	4200
5997.98	$4f^7 5d 6s^2$	$^7D_5^0$	6976.508	$4f^7 5d 6s 6p$	$J=4$	23 644.156	4400
5999.06	$4f^7 5d^2 6s$	$^{11}F_3^0$	6550.395	$4f^7 5d 6s 6p$	$J=2$	23 215.028	4200

pole moments of the odd-A isotopes ^{155,157}Gd, the electric quadrupole hfs is comparable to the magnetic dipole for many of the levels studied. For these reasons, analysis of the observed hfs patterns was difficult; the final interpretation for each line is unique, however, and rough values (to within ~ 3 MHz) for the lower-state hfs intervals were obtained in this way before making laser-rf double-resonance studies.

Once the identification of the individual hfs components was known, the laser-rf double-resonance method, as described above, was used to determine the lower-state splittings precisely. This information could then be used to refine the values of the upper-state splittings determined from the fluorescence spectra. It is worth noting that although the rf measurements yield the lower-state $\Delta\nu$ values with great precision, they are completely insensitive to the sign (level ordering), and this information must come from the fluorescence spectra.

The degree of depopulation produced by the pump beam was at least 50% for all of the lines studied except for those for which the lower level is in the $4f^8 6s^2$ configuration. Figure 2 shows a typical double-resonance observation; it shows the $\sim 50\%$ increase in fluorescence observed when the rf is tuned to the $F = \frac{9}{2} \leftrightarrow \frac{7}{2}$ interval in the $^{11}F_3$ level of ^{157}Gd.

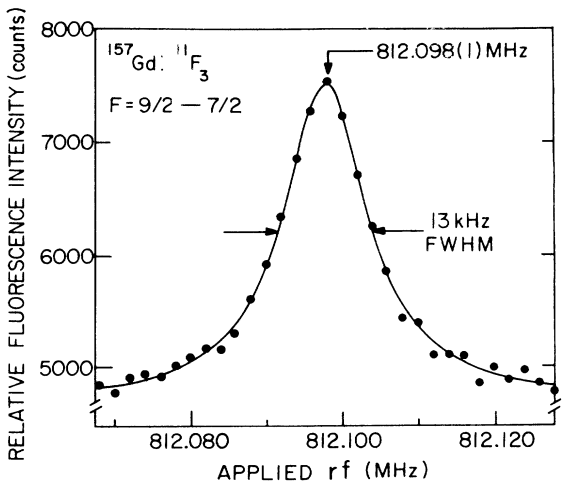

FIG. 2. Example of a laser-rf double-resonance signal, showing the resonant increase in fluorescence when the rf is tuned to resonance with the $F = \frac{9}{2} \leftrightarrow \frac{7}{2}$ hfs interval in the $^{11}F_3$ level of ^{157}Gd. Lower-state hfs splittings are easily determined to ± 1 kHz from such observations.

TABLE II. hfs intervals measured for metastable levels of ^{155,157}Gd I by laser-rf double resonance. The signs (i.e., the level orderings) are from analysis of the fluorescence patterns as explained in the text. The uncertainties are ± 1 kHz.

Excitation energy (cm^{-1})	Configuration	State	$F-F'$	Measured hfs interval $\Delta\nu$ (MHz) ^{155}Gd	^{157}Gd
6378.146	$4f^7 5d^2 6s$	$^{11}F_2$	3.5–2.5	−539.650	−724.933
			2.5–1.5	−479.244	−617.726
			1.5–0.5	−325.065	−410.610
6550.395	$4f^7 5d^2 6s$	$^{11}F_3$	4.5–3.5	−633.290	−812.098
			3.5–2.5	−395.134	−527.849
			2.5–1.5	−230.037	−321.424
6786.184	$4f^7 5d^2 6s$	$^{11}F_4$	5.5–4.5	−675.153	−859.774
			4.5–3.5	−426.890	−569.747
			3.5–2.5	−253.927	−359.939
7103.420	$4f^7 5d^2 6s$	$^{11}F_5$	6.5–5.5	−634.168	−815.874
			5.5–4.5	−461.088	−609.929
			4.5–3.5	−325.749	−444.175
7480.348	$4f^7 5d^2 6s$	$^{11}F_6$	7.5–6.5	−689.214	−896.016
			6.5–5.5	−558.555	−735.244
			5.5–4.5	−444.506	−592.179
7947.294	$4f^7 5d^2 6s$	$^{11}F_7$	8.5–7.5	−658.442	−876.774
			7.5–6.5	−635.794	−832.022
			6.5–5.5	−592.595	−765.375
8498.434	$4f^7 5d^2 6s$	$^{11}F_8$	9.5–8.5	−600.103	−829.235
			8.5–7.5	−717.275	−934.071
			7.5–6.5	−774.340	−974.875
6976.508	$4f^7 5d 6s^2$	$^7D_5$	6.5–5.5	187.592	173.368
			5.5–4.5	−173.957	−207.703
			4.5–3.5	−369.172	−411.589
7562.457	$4f^7 5d 6s^2$	$^7D_2$	3.5–2.5	−203.458	−209.612
			2.5–1.5	186.568	203.843
			1.5–0.5		263.770

Precise double-resonance measurements were made of the hyperfine intervals in the seven levels of $4f^7 5d^2 6s\ ^{11}F_{2-8}$, and of those in the levels of $4f^7 5d 6s^2\ ^7D_{2,5}$ for both ^{155}Gd and ^{157}Gd. The measured intervals are listed in Table II. The measurements have an uncertainty of ± 1 kHz.

In addition to the studies of transitions from the $4f^7 5d^2 6s$ and $4f^7 5d 6s^2$ configurations already described, efforts were made to make corresponding studies on lines from the $4f^8 6s^2\ ^7F$ term at 11 000–15 000 cm^{-1} excitation. No such lines in a convenient wavelength region were known to us, but consideration of the properties of known levels[1] identified a number of possible lines. Careful laser scans at 19 such wavelengths showed two very weak lines (at 5868.89 and 5739.17 Å) from the $4f^8 6s^2\ ^7F_6$ level at 10 947.21 cm^{-1}; no other lines from the ^7F term were found. The two lines mentioned showed strong components arising from the abundant even-A isotopes ^{156,158,160}Gd, but only the $\Delta F = \Delta J$ components could be seen from the odd-A ^{155,157}Gd. Our inability to detect the $\Delta F = \Delta J \pm 1$ hfs components (the so-called "off-diagonal" lines) was a serious obstacle to measurement of the hfs of the $4f^8 6s^2\ ^7F$ levels. Even worse, however, was the discovery that the pump beam achieved almost no ($<5\%$) population depletion. This is probably due to very weak intrinsic line strengths. Although the isotope shifts could be measured for the line at 5868.89 Å for the even-A isotopes, it was not possible to obtain even crude measurements for the upper- and lower-state hfs of the odd-A isotopes.

III. RESULTS AND ANALYSIS

The magnetic dipole (A) and electric quadrupole (B) hyperfine constants can be determined from the measured zero-field hfs intervals. For the upper states of the optical transitions the hfs intervals were obtained from analysis of the laser fluorescence patterns using the 150-MHz frequency markers for calibration. This information was also available for the lower levels and was used to obtain the signs and preliminary values of the magnitudes of the hfs intervals. The precise intervals determined by laser-rf double-resonance and displayed in Table II were used for the final evaluation of the lower-state hfs constants. The standard first-order theory[10] of atomic hyperfine structure was used in extracting the A and B values from the observed hfs intervals. Because the nuclear spin of both ^{155}Gd and ^{157}Gd is $I = \frac{3}{2}$, all of the states studied have four hfs levels and therefore three zero-field intervals. In fitting the three intervals for each state with the two adjustable parameters A and B, the residuals (for the states studied by rf) were typically 1–4 kHz. For the upper states (for which rf data were not available) the corresponding residuals were typically 3–4 MHz.

For each line studied the hfs constants could be evaluated for each of the odd-A isotopes ^{155}Gd and ^{157}Gd. As described below, the ratios $A(^{157}\text{Gd})/A(^{155}\text{Gd})$ and $B(^{157}\text{Gd})/B(^{155}\text{Gd})$ were level independent to within the precision of the fluorescence data, and this was used in some cases to aid in evaluating the upper-state hfs constants. For the lower states, the precision of the rf measurements allowed determination of these ratios as discussed below. Some of the optical lines studied terminate in a common upper state, and in these cases the upper-state splittings could be determined more accurately.

Table III lists the hfs constants determined for the upper levels by laser fluorescence spectroscopy. The precision is ± 0.4 MHz for the A values (except for the level at 23 103 cm^{-1}, for which it is ± 1.0 MHz), and ± 8 MHz for the B values. The lines used for the determination are given in the right-hand column. Table IV lists the values found by double resonance for the hfs constants for the lower levels. The precision is ± 0.002 MHz for the A values and ± 0.020 MHz for the B values. Second-order hfs interactions have not been included; the A and B values given are those needed to reproduce the observed

TABLE III. Magnetic dipole (A) and electric quadrupole (B) hfs constants in MHz determined for highly excited ^{155,157}Gd levels by Doppler-free laser fluorescence spectroscopy. The optical lines used in the study are listed in the right-hand column. The uncertainties are ± 0.4 MHz for the A values (except for the level at 23 103 cm^{-1}, for which it is ± 1 MHz) and ± 8 MHz for the B values.

Level energy (cm^{-1})	^{155}Gd A	^{155}Gd B	^{157}Gd A	^{157}Gd B	Lines used (Å)
23 103.660	136.3	59	174.6	65	5977.23
23 215.028	28.4	−219	38.0	−233	5999.06
					5937.70
23 389.782	2.3	−295	2.3	−312	5936.80
23 644.156	−7.6	−248	−9.2	−266	5930.27
					5997.98
23 999.912	−10.6	−78	−13.6	−80	5916.75
					5807.70
24 458.988	239.3	−4	313.7	−4	5916.73
24 849.514	−39.9	103	−52.5	102	5633.48
24 854.297	−72.5	521	−95.0	555	5754.14
25 043.649	−28.9	412	−37.9	439	5692.10
25 376.313	−6.7	592	−8.5	632	7535.96
					5923.26

TABLE IV. hfs constants in MHz determined from laser-rf double resonance for metastable levels in ^{155,157}Gd. The signs are determined from analysis of the laser fluorescence patterns as explained in the text. The uncertainties are ±2 kHz for the A values and ±20 kHz for the B values. The values given are not corrected for second-order hfs; they are the values required to reproduce the observed hfs splittings using the standard first-order theory.

Level energy		^{155}Gd		^{157}Gd	
(cm^{-1})	S,L,J	A	B	A	B
6378.146	$^{11}F_2$	−172.942	75.027	−227.108	79.937
6550.395	$^{11}F_3$	−123.333	−104.390	−161.933	−111.204
6786.184	$^{11}F_4$	−103.231	−156.191	−135.524	−166.390
7103.420	$^{11}F_5$	−87.266	−102.989	−114.551	−109.688
7480.348	$^{11}F_6$	−87.209	−56.231	−114.476	−59.908
7947.294	$^{11}F_7$	−83.402	83.141	−109.476	88.574
8498.434	$^{11}F_8$	−80.849	282.893	−106.124	301.379
6976.508	$^{7}D_5$	−16.507	453.674	−21.656	483.282
7562.457	$^{7}D_2$	8.248	−265.516	10.827	−282.870

hfs intervals of Table II using the standard first-order theory. The structure of the Gd atom is complex, and it must be understood better before second-order hfs corrections can be relied on.

As noted above, study of the laser fluorescence scans permits determination of the shifts between the various isotopes present in the atomic beam. Although this is straightforward for the even-A isotopes, the corresponding values for the odd-A isotopes require determination of the "center of gravity" for the various hfs components due to each isotope. This is possible only after a detailed analysis of the hfs pattern has positively identified all of the observed hfs components in a laser scan. The isotope-shift values resulting from these studies are presented in Table V. All of the observed shifts are negative, reflecting the fact that the wavelength observed for the heavier isotopes is to the red of that for the lighter. The uncertainties are ±4 MHz. If one considers the ^{160}Gd-^{158}Gd shifts as representative, it is found that its value for the lines with $4f^75d^26s\,^{11}F$ lower levels range from −376 to −483 MHz except for the lines to the $^{11}F_6$ level, for which the shift is about 50% greater. For the lines connecting with the $^{7}D_{2,5}$ levels of $4f^75d6s^2$ the corresponding shifts are much larger, especially for the $^{7}D_5$ level. A large shift is also found for the only line studied that connects with the $4f^86s^2\,^7F$ term.

Table VI lists the isotopic ratios found for the hfs constants for each state studied by double resonance. The values observed previously[4] for the atomic ground state are included for comparison. It is seen that within the $^{11}F_J$ term there is a clear J dependence for the dipole ratio, with the larger values associated with the smaller-J values. Because of the noncontact nature of the electric quadrupole hfs, the ratios of the quadrupole hfs constants show no evidence of state-to-state variation.

The departure of the ratio of the dipole hfs constants

TABLE V. Isotope shifts observed in the course of the hfs measurements. The negative signs indicate that in each case the lighter isotope lies at a higher laser frequency than the heavier. The uncertainties are ±4 MHz.

Observed wavelength	Isotope shifts (MHz)					
(Å)	160–158	158–156	156–154	154–152	158–157	156–155
5633.48	−377	−355	−488	−1087	−288	−248
5692.10	−562	−541	−766	−1925	−487	−395
5735.96	−441	−440	−569	−1362	−363	−289
5754.14	−688	−646	−943	−2467	−605	−488
5807.70	−376	−359	−481		−288	−247
5868.90	−974	−941				
5872.64	−1648	−1592	−2129		−1300	−1093
5916.73	−1032	−995	−1332		−805	−681
5916.75	−452	−438	−584		−359	−298
5923.26	−459	−445	−599	−1402	−371	−305
5930.27	−421	−412	−529		−320	−271
5936.80	−445	−427	−559		−338	−287
5937.70	−455	−443	−591		−354	−302
5977.23	−483	−459	−604		−363	−304
5997.98	−1696	−1641	−2188		−1330	−1116
5999.06	−467	−443	−592		−352	−303

TABLE VI. Isotopic ratios observed for the dipole and quadrupole hfs constants of ^{155,157}Gd. The previously measured (Ref. 4) ground-state values are included for comparison. The excited-state dipole values show a J-dependent (and term-dependent) hfs anomaly relative to the ground-state value. No such variation is found for the quadrupole interaction.

Excitation energy (cm^{-1})	S,L,J	hfs ratios $A(^{157}Gd)/A(^{155}Gd)$	$B(^{157}Gd)/B(^{155}Gd)$
0	$^9D_2$	1.311 24	1.065 5
6378	$^{11}F_2$	1.313 20(5)	1.065 4(5)
6550	$^{11}F_3$	1.312 97(5)	1.065 3(5)
6786	$^{11}F_4$	1.312 82(5)	1.065 3(5)
7103	$^{11}F_5$	1.312 66(5)	1.065 0(5)
7480	$^{11}F_6$	1.312 66(5)	1.065 4(5)
7947	$^{11}F_7$	1.312 63(5)	1.065 3(5)
8498	$^{11}F_8$	1.312 62(5)	1.065 4(5)
6976	$^7D_5$	1.311 9(2)	1.065 3(5)
7562	$^7D_2$	1.312 6(6)	1.065 4(5)

from the ratio of the nuclear magnetic dipole moments (for two isotopes of the same I) is often used[11] to define a hyperfine anomaly Δ. For ^{155,157}Gd, we may write

$$^{155,157}\Delta = \frac{A(^{155}Gd)}{A(^{157}Gd)}\frac{\mu(^{157}Gd)}{\mu(^{155}Gd)} - 1 .$$

Although the moment ratio $\mu(^{157}Gd)/\mu(^{155}Gd)$ is not known[2] for Gd with precision comparable to that for the ratios of the hfs constants, it is clear that there is a definite hfs anomaly (relative to the atomic ground state) throughout the ^{11}F term of $4f^7 5d^2 6s$.

IV. DISCUSSION

Although one would very much like to compare the hfs constants measured for the (relatively pure) lower levels of ^{155,157}Gd with *ab initio* values, it is not yet possible to make such calculations in the middle of the $4f$ shell. One can, however, make useful comparisons with predictions of the Sandars-Beck effective-operator method.[12] Calculations of this type should be especially reliable for the ^{11}F term of $4f^7 5d^2 6s$ because all of the levels of the term are reported[1] to be 98–99% pure L-S coupled states. The purity of the previously studied ground term, by comparison, is reported[4] to be only 92–95%. Thus for the ^{11}F term errors due to admixture are expected to be minimal.

General expressions for the A and B values of L-S coupled states arising from three open shells have not been published but can be derived in a straightforward way from the effective hfs Hamiltonian of Sandars and Beck following the rules of Racah algebra. The expressions are given in the Appendix because they are extremely general and consequently may be of use to others in the future. Because there are three open shells, the expression for each A or B would normally be a linear combination of nine radial integrals (three for each shell). For the $4f^7 5d^2 6s\ ^{11}F$ levels, however, this reduces for the A values to three due to the following: (1) the half-filled ^8S nature of the $4f$ shell, (2) one of the shells contains only an s electron, and (3) although all three shells contribute contact hfs, the linear combination of the three is independent of J (within ^{11}F) and can be represented by a single radial integral. Thus the expressions for the A values of the seven states can be given in the L-S limit in terms of three radial integrals a^{01}_{5d}, a^{12}_{5d}, and A^{10} (defined in the Appendix), which we will treat as adjustable parameters. We obtain

$$A(^{11}F_8) = 0.3750a^{01}_{5d} - 0.0179a^{12}_{5d} + 0.1250A^{10} ,$$
$$A(^{11}F_7) = 0.3393a^{01}_{5d} + 0.0015a^{12}_{5d} + 0.1321A^{10} ,$$
$$A(^{11}F_6) = 0.2857a^{01}_{5d} + 0.0163a^{12}_{5d} + 0.1429A^{10} ,$$
$$A(^{11}F_5) = 0.2000a^{01}_{5d} + 0.0251a^{12}_{5d} + 0.1600A^{10} ,$$
$$A(^{11}F_4) = 0.0500a^{01}_{5d} + 0.0249a^{12}_{5d} + 0.1900A^{10} ,$$
$$A(^{11}F_3) = -0.2500a^{01}_{5d} + 0.0071a^{12}_{5d} + 0.2500A^{10} ,$$
$$A(^{11}F_2) = -1.0000a^{01}_{5d} - 0.0571a^{12}_{5d} + 0.4000A^{10} .$$

These expressions may be equated to the measured A values in Table IV for the ^{11}F levels of ^{155,157}Gd. When a least-squares fit is made for ^{157}Gd, for example, the rms value for the residuals A^{obs}-A^{calc} is 2.5 MHz, indicating a rather good fit. The residual for the $J=5$ level, however, is 2.4 times larger than that for any other level. If one omits the $J=5$ level from the fit the rms residual drops to 0.07 MHz, while the residual for the $J=5$ level increases to 7.7 MHz, indicating that the hfs of the $J=5$ state is strongly perturbed compared with that for the other J's.

The expressions for the B values of the $^{11}F_J$ levels also contain only three radial integrals b^{02}_{5d}, b^{13}_{5d}, and b^{11}_{5d}. The lack of dependence on the $4f$ and $6s$ shells is due to the fact that for the ^{11}F states each of these shells has $L=0$ and consequently no electric quadrupole hfs interaction.

The effective-operator expressions for the B values of the ^{11}F levels are

$$B(^{11}F_8)=0.2857b^{02}_{5d}+0.0350b^{13}_{5d}+0.2000b^{11}_{5d}\ ,$$

$$B(^{11}F_7)=0.1071b^{02}_{5d}-0.0289b^{13}_{5d}+0.1683b^{11}_{5d}\ ,$$

$$B(^{11}F_6)=-0.0327b^{02}_{5d}-0.0360b^{13}_{5d}+0.1371b^{11}_{5d}\ ,$$

$$B(^{11}F_5)=-0.1275b^{02}_{5d}-0.0118b^{13}_{5d}+0.1046b^{11}_{5d}\ ,$$

$$B(^{11}F_4)=-0.1652b^{02}_{5d}+0.0195b^{13}_{5d}+0.0672b^{11}_{5d}\ ,$$

$$B(^{11}F_3)=-0.1190b^{02}_{5d}+0.0321b^{13}_{5d}+0.0167b^{11}_{5d}\ ,$$

$$B(^{11}F_2)=0.0816b^{02}_{5d}-0.0120b^{13}_{5d}-0.0686b^{11}_{5d}\ .$$

Just as for the A values, these expressions may be equated to the experimental B values for either ^{155}Gd or ^{157}Gd. When this is done for ^{157}Gd, for example, adjustment of the three radial parameters $b^{k,k'}_{5d}$ to obtain a least-squares fit results in a rms residual of 11 MHz. The residual for the $J=5$ level is more than twice as large as that for any other J, just as was found in the fit to the A values. If the $J=5$ level is omitted from the fit, the rms residual drops to 1.6 MHz while the residual for $J=5$ increases to 34 MHz. Thus the fits of the effective-operator theoretical expressions for the A and B values independently point strongly to a substantial admixture in the $J=5$ level while the other J's appear to be relatively near the (single-configuration) L-S limit. The nature of the perturbation and resulting admixture will be discussed below.

The values found from these fits for the radial integrals for ^{157}Gd are

$$a^{01}_{5d}=-51.0\pm0.5\ \text{MHz}\ ,$$

$$a^{12}_{5d}=-17\pm5\ \text{MHz}\ ,$$

$$A^{10}=-698\pm2\ \text{MHz}\ ,$$

$$b^{02}_{5d}=1038\pm30\ \text{MHz}\ ,$$

$$b^{13}_{5d}=470\pm10\ \text{MHz}\ ,$$

$$b^{11}_{5d}=-57\pm14\ \text{MHz}\ .$$

The corresponding values for ^{155}Gd may be obtained by dividing the above by the isotopic ratios in Table VI. The values found for most of the radial parameters in the $4f^75d^26s\,^{11}F$ term are rather close to the corresponding values reported[4] for the ground ^9D term of $4f^75d6s^2$. The finding that a^{01}_{5d} is much larger than a^{12}_{5d} is in agreement with the ground-term results. The A^{10} value is substantially larger in the $4f^75d^26s$ configuration, however, because of the large contribution of the unpaired $6s$ electron. The ratios b^{13}_{5d}/b^{02}_{5d} and b^{11}_{5d}/b^{02}_{5d} found for the $4f^75d^26s$ term are rather similar to those evaluated[13] for $5d$-shell atoms (with a filled $4f$ shell).

The admixture in the $^{11}F_5$ level that causes its hfs to be inconsistent with the predictions of the effective-operator theory is apparently not due to spin-orbit mixing within the $4f^75d^26s$ configuration. Previous study has revealed[1] that the ^{11}F levels are rather close to the L-S coupling scheme

$$4f^7(^8S)5d^2(^3F)(^{10}F)6s\ ^{11}F_J\ ,$$

TABLE VII. hfs constants of two admixed $J=5$ levels in ^{157}Gd. The observed values are given in the inner columns (3 and 4) and the values predicted from the effective-operator treatment described in the text in the outer columns (2 and 5). The observed values lie between the predicted ones in all cases, indicating an admixture on the order of 5%.

	State 1 $4f^75d^26s\,^{11}F_5$		State 2 $4f^75d6s^2\,^7D_5$	
	Predicted	Observed	Observed	Predicted
A	−122	−114.6	−21.7	−19.5
B	−144	−109.7	+483	+611

and in addition there is no obvious reason to suppose the degree of intermediate coupling in the $J=5$ level to be substantially different from that for the $J\neq5$ levels. That the ^{11}F levels (with the possible exception of that for $J=5$) do not have substantial spin-orbit mixing is also shown by the remarkable success of the effective-operator theory (based on the L-S limit picture) in accounting for the hfs. It is speculated that the admixture in the $J=5$ level is instead caused by (Coulomb) configuration interaction with the very close (127 cm^{-1}) $4f^75d6s^2\,^7D_5$ level at 6976 cm^{-1} excitation. The hfs constants for this level may be predicted (in the L-S limit) from the effective-operator theory and the parameter values found above to be $A^{\text{pred}}=-19$ MHz and $B^{\text{pred}}=+611$ MHz. (The measured values are given in Table IV.) Thus even a small admixture of this state into the $^{11}F_5$ state could be expected to alter the hfs constants of the $^{11}F_5$ level considerably. It is found that the A and B values measured

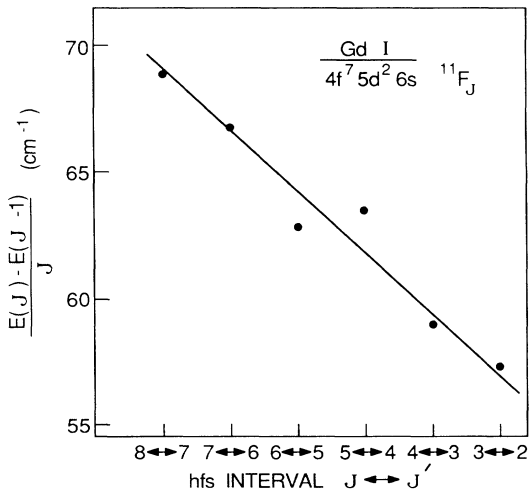

FIG. 3. Plot of the fine-structure spacings E_J-E_{J-1} divided by the J value of the upper level plotted against J for the $^{11}F_J$ term of $4f^75d^26s$. The departure of the $J=6\leftrightarrow5$ and $5\leftrightarrow4$ intervals from the straight line through the other data points strongly suggests that the $J=5$ level is perturbed relative to the other members of the multiplet. The perturbing state is believed to be the $^7D_5$ level of $4f^75d6s^2$, which lies only 127 cm^{-1} away.

for the $^{11}F_5$ level ($A^{\rm obs} = -114.6$ MHz, $B^{\rm obs} = -109.7$ MHz) are in fact shifted from the predicted values ($A^{\rm pred} = -122$ MHz, $B^{\rm pred} = -144$ MHz) in a direction consistent with such an admixture. Interpretation of the observed hfs of the $^7D_5$ level is more difficult because of its much greater departure[1] from the L-S limit. The results are summarized in Table VII. The degree of admixture appears to be about 5%.

The perturbation of the $4f^7 5d^2 6s\ ^{11}F_5$ level can also be seen by considering the fine-structure splitting within the ^{11}F term. Figure 3 shows a plot of $(E_J - E_{J-1})/J$ versus J for the levels of this term. The points lie on a straight line except for the two intervals $J = 6 \leftrightarrow 5$ and $J = 5 \leftrightarrow 4$, indicating that the position of the $J = 5$ level within the multiplet is indeed perturbed. Thus both the fine and hyperfine structure indicate substantial perturbation of the $J = 5$ member of the ^{11}F term.

Calculating the degree of admixture from *ab initio* considerations is unfortunately extremely difficult[14] because of the complexity of the configurations involved.

V. CONCLUSIONS

The low-lying electronic states of the gadolinium atom are derived from a nearly half-filled $4f$ electron shell plus a few additional electrons in the $5d$ or $6s$ shell. The resulting configurations are therefore extremely complex and remain beyond the present capabilities of accurate *ab initio* calculation. This paper shows that in spite of this complexity a surprisingly quantitative understanding can be achieved for the hyperfine structure through use of the effective-operator formalism of Sandars and Beck. Even levels built from three open electron shells show remarkable consistency with the theory, as illustrated by the ^{11}F term of the $4f^7 5d^2 6s$ configuration. The values found for the hfs radial integrals, such as the $a_{nl}^{k_s k_l}$ and $b_{nl}^{k_s k_l}$, depend only weakly on the particular electron configuration (or multiplet therein) from which they are evaluated. Hopefully a rather broad systematic understanding of the hyperfine structure of such complex atoms is not too far off, although full realization of this goal depends critically on further development of *ab initio* calculational capability.

The perturbation found between the $J = 5$ levels of the terms $4f^7 5d^2 6s\ ^{11}F$ and $4f^7 5d 6s^2\ ^7D$ shows up strikingly in both the fine and hyperfine structure, and illustrates that some degree of understanding is already possible for limited aspects of this extremely complicated many-electron system. It is unfortunate that the *ab initio* theory is not yet able to address this problem.

ACKNOWLEDGMENTS

This research was supported by the U. S. Department of Energy, Office of Basic Energy Sciences, under Contract No. W-31-109-ENG-38.

APPENDIX

Based on the effective-operator hyperfine Hamiltonian of Sandars and Beck, L-S limit expressions have been published[10,15] for the magnetic dipole (A) and electric quadrupole (B) hfs constants of states of l^N or $l^N l'$ configurations. The $4f^7 5d^2 6s\ ^{11}F$ multiplet considered in this work requires more general expressions capable of treating states built from three open electron shells. Because such states are sure to be studied in the future, it appears worthwhile to give these general expressions here. We consider the general case of three open shells, each denoted by

$$(n_i l_i)^{N_i} \alpha_i S_i L_i = \Psi_i$$

coupled stepwise $(\Psi_1, \Psi_2)\Psi_{12}$ and $(\Psi_{12}, \Psi_3)\Psi$ to form the final L-S coupled state

$$\Psi = |[(l_1^{N_1} \alpha_1 S_1 L_1, l_2^{N_2} \alpha_2 S_2 L_2) S_{12} L_{12}, l_3^{N_3} \alpha_3 S_3 L_3] SLJ\rangle = |(\Psi_1, \Psi_2)\Psi_{12}, \Psi_3; \Psi_J\rangle$$

in which we require that $n_1 l_1$, $n_2 l_2$ and $n_3 l_3$ be distinct shells. We evaluate the diagonal matrix element between these states

$$\langle (\Psi_1, \Psi_2)\Psi_{12}, \Psi_3; SLJIFM | H_{\rm hfs} | (\Psi_1, \Psi_2)\Psi_{12}, \Psi_3; SLJIFM \rangle$$

and extract expressions for the A and B values of the state $|\tau SLJ\rangle$. We obtain for the magnetic dipole hfs constant A

$$\begin{aligned} A(\Psi_J) = {} & [J(J+1)(2J+1)]^{-1/2} \\ & \times \left[(-1)^{S+L+J+L_{12}} (2J+1)(2L+1) \begin{Bmatrix} J & J & 1 \\ L & L & S \end{Bmatrix} \right. \\ & \quad \times \left[(-1)^{L_3+L+L_1+1} \begin{Bmatrix} L & L & 1 \\ L_{12} & L_{12} & L_3 \end{Bmatrix} (2L_{12}+1) \right. \\ & \quad\quad \times \left[a^{01}_{n_1 l_1} (-1)^{L_2+L_{12}} [L_1(L_1+1)(2L_1+1)]^{1/2} \begin{Bmatrix} L_{12} & L_{12} & 1 \\ L_1 & L_1 & L_2 \end{Bmatrix} \right. \\ & \quad\quad\quad \left. \left. \left. + a^{01}_{n_2 l_2} (-1)^{L_2+L_{12}} [L_2(L_2+1)(2L_2+1)]^{1/2} \begin{Bmatrix} L_{12} & L_{12} & 1 \\ L_2 & L_2 & L_1 \end{Bmatrix} \right] \right] \end{aligned}$$

$$+a^{01}_{n_3l_3}(-1)^{L_3+L}[L_3(L_3+1)(2L_3+1)]^{1/2}\begin{Bmatrix}L & L & 1\\ L_3 & L_3 & L_{12}\end{Bmatrix}\Bigg]$$

$$+(-1)^{S+L+J}(2J+1)(2S+1)\begin{Bmatrix}J & J & 1\\ S & S & L\end{Bmatrix}(-1)^{S_{12}}$$

$$\times\Bigg[(-1)^{S_3+S+S_1+1}\begin{Bmatrix}S & S & 1\\ S_{12} & S_{12} & S_3\end{Bmatrix}(2S_{12}+1)$$

$$\times\Bigg[a^{10}_{n_1l_1}(-1)^{S_2+S_{12}}[S_1(S_1+1)(2S_1+1)]^{1/2}\begin{Bmatrix}S_{12} & S_{12} & 1\\ S_1 & S_1 & S_2\end{Bmatrix}$$

$$+a^{10}_{n_2l_2}(-1)^{S_2+S_{12}}[S_2(S_2+1)(2S_2+1)]^{1/2}\begin{Bmatrix}S_{12} & S_{12} & 1\\ S_2 & S_2 & S_1\end{Bmatrix}\Bigg]$$

$$+a^{10}_{n_3l_3}(-1)^{S_3+S}[S_3(S_3+1)(2S_3+1)]^{1/2}\begin{Bmatrix}S & S & 1\\ S_3 & S_3 & S_{12}\end{Bmatrix}\Bigg]$$

$$-(30)^{1/2}(2S+1)(2L+1)(2J+1)\begin{Bmatrix}S & S & 1\\ L & L & 2\\ J & J & 1\end{Bmatrix}(-1)^{S_{12}+L_{12}}$$

$$\times\Bigg[(-1)^{S_3+L_3+S+L}\begin{Bmatrix}S & S & 1\\ S_{12} & S_{12} & S_3\end{Bmatrix}\begin{Bmatrix}L & L & 2\\ L_{12} & L_{12} & L_3\end{Bmatrix}(-1)^{S_1+L_1+1}(2S_{12}+1)(2L_{12}+1)$$

$$\times\Bigg[a^{12}_{n_1l_1}(-1)^{S_2+L_2+S_{12}+L_{12}}\begin{Bmatrix}S_{12} & S_{12} & 1\\ S_1 & S_1 & S_2\end{Bmatrix}\begin{Bmatrix}L_{12} & L_{12} & 2\\ L_1 & L_1 & L_2\end{Bmatrix}$$

$$\times\left[\frac{l_1(l_1+1)(2l_1+1)}{(2l_1-1)(2l_1+3)}\right]^{1/2}\langle l_1^{N_1}\alpha_1S_1L_1\|V^{(12)}\|l_1^{N_1}\alpha_1S_1L_1\rangle$$

$$+a^{12}_{n_2l_2}(-1)^{S_2+L_2+S_{12}+L_{12}}\begin{Bmatrix}S_{12} & S_{12} & 1\\ S_2 & S_2 & S_1\end{Bmatrix}\begin{Bmatrix}L_{12} & L_{12} & 2\\ L_2 & L_2 & L_1\end{Bmatrix}$$

$$\times\left[\frac{l_2(l_2+1)(2l_2+1)}{(2l_2-1)(2l_2+3)}\right]^{1/2}\langle l_2^{N_2}\alpha_2S_2L_2\|V^{(12)}\|l_2^{N_2}a_2S_2L_2\rangle\Bigg]$$

$$+a^{12}_{n_3l_3}(-1)^{S_3+L_3+S+L}\begin{Bmatrix}S & S & 1\\ S_3 & S_3 & S_{12}\end{Bmatrix}\begin{Bmatrix}L & L & 2\\ L_3 & L_3 & L_{12}\end{Bmatrix}$$

$$\times\left[\frac{l_3(l_3+1)(2l_3+1)}{(2l_3-1)(2l_3+3)}\right]^{1/2}\langle l_3^{N_3}\alpha_3S_3L_3\|V^{(12)}\|l_3^{N_3}\alpha_3S_3L_3\rangle\Bigg]\Bigg].$$

The quantities $a^{k_sk_l}_{n_il_i}$ are the radial integrals required by the Sandars-Beck theory and are sometimes treated as adjustable parameters. Similarly, we obtain for the electric quadrupole hfs B value

$$B(\Psi_J)=\left[\frac{4J(2J-1)(2J+1)}{(J+1)(2J+3)}\right]^{1/2}$$

$$\times\Bigg[(-1)^{S+L+J}\begin{Bmatrix}L & L & 2\\ J & J & S\end{Bmatrix}(-1)^{L_{12}+L_3+L}(2L+1)$$

$$\times\Bigg[(2L_{12}+1)(-1)^{L_1+L_2+L_{12}}\begin{Bmatrix}L & L & 2\\ L_{12} & L_{12} & L_3\end{Bmatrix}$$

$$\times\Bigg[\left[\frac{l_1(l_1+1)(2l_1+1)}{(2l_1-1)(2l_1+3)}\right]^{1/2}b^{02}_{n_1l_1}\begin{Bmatrix}L_{12} & L_{12} & 2\\ L_1 & L_1 & L_2\end{Bmatrix}\langle l_1^{N_1}\alpha_1S_1L_1\|U^{(2)}\|l_1^{N_1}\alpha_1S_1L_1\rangle$$

$$
\begin{aligned}
&+\left[\frac{l_2(l_2+1)(2l_2+1)}{(2l_2-1)(2l_2+3)}\right]^{1/2} b^{02}_{n_2 l_2}
\begin{Bmatrix} L_{12} & L_{12} & 2 \\ L_2 & L_2 & L_1 \end{Bmatrix}
\langle l_2^{N_2}\alpha_2 S_2 L_2 \| U^{(2)} \| l_2^{N_2}\alpha_2 S_2 L_2\rangle \Bigg] \\
&+\left[\frac{l_3(l_3+1)(2l_3+1)}{(2l_3-1)(2l_3+3)}\right]^{1/2} b^{02}_{n_3 l_3}
\begin{Bmatrix} L & L & 2 \\ L_3 & L_3 & L_{12} \end{Bmatrix}
\langle l_3^{N_3}\alpha_3 S_3 L_3 \| U^{(2)} \| l_3^{N_3}\alpha_3 S_3 L_3\rangle \Bigg] \\
&+(-1)^{S_{12}+L_{12}+S_3+L_3+S+L}
\begin{Bmatrix} S & S & 1 \\ L & L & 3 \\ J & J & 2 \end{Bmatrix}(2S+1)(2L+1) \\
&\times\Bigg[\begin{Bmatrix} S & S & 1 \\ S_{12} & S_{12} & S_3 \end{Bmatrix}(-1)^{S_1+L_1+S_2+L_2+S_{12}+L_{12}}(2S_{12}+1)(2L_{12}+1) \\
&\quad\times\begin{Bmatrix} L & L & 3 \\ L_{12} & L_{12} & L_3 \end{Bmatrix}\Bigg[\begin{Bmatrix} S_{12} & S_{12} & 1 \\ S_1 & S_1 & S_2 \end{Bmatrix}\begin{Bmatrix} L_{12} & L_{12} & 3 \\ L_1 & L_1 & L_2 \end{Bmatrix} \\
&\qquad\times b^{13}_{n_1 l_1}\langle l_1^{N_1}\alpha_1 S_1 L_1 \| V^{(13)} \| l_1^{N_1}\alpha_1 S_1 L_1\rangle \\
&\qquad+\begin{Bmatrix} S_{12} & S_{12} & 1 \\ S_2 & S_2 & S_1 \end{Bmatrix}\begin{Bmatrix} L_{12} & L_{12} & 3 \\ L_2 & L_2 & L_1 \end{Bmatrix} b^{13}_{n_2 l_2}\langle l_2^{N_2}\alpha_2 S_2 L_2 \| V^{(13)} \| l_2^{N_2}\alpha_2 S_2 L_2\rangle \Bigg] \\
&\quad+b^{13}_{n_3 l_3}\begin{Bmatrix} S & S & 1 \\ S_3 & S_3 & S_{12} \end{Bmatrix}\begin{Bmatrix} L & L & 3 \\ L_3 & L_3 & L_{12} \end{Bmatrix}\langle l_3^{N_3}\alpha_3 S_3 L_3 \| V^{(13)} \| l_3^{N_3}\alpha_3 S_3 L_3\rangle \Bigg] \\
&+(-1)^{S_{12}+L_{12}+S_3+L_3+S+L}
\begin{Bmatrix} S & S & 1 \\ L & L & 1 \\ J & J & 2 \end{Bmatrix}(2S+1)(2L+1) \\
&\times\Bigg[\begin{Bmatrix} S & S & 1 \\ S_{12} & S_{12} & S_3 \end{Bmatrix}\begin{Bmatrix} L & L & 1 \\ L_{12} & L_{12} & L_3 \end{Bmatrix}(-1)^{S_1+L_1+S_2+L_2+S_{12}+L_{12}}(2S_{12}+1)(2L_{12}+1) \\
&\quad\times\Bigg[b^{11}_{n_1 l_1}\begin{Bmatrix} S_{12} & S_{12} & 1 \\ S_1 & S_1 & S_2 \end{Bmatrix}\begin{Bmatrix} L_{12} & L_{12} & 1 \\ L_1 & L_1 & L_2 \end{Bmatrix}\langle l_1^{N_1}\alpha_1 S_1 L_1 \| V^{(11)} \| l_1^{N_1}\alpha_1 S_1 L_1\rangle \\
&\qquad+b^{11}_{n_2 l_2}\begin{Bmatrix} S_{12} & S_{12} & 1 \\ S_2 & S_2 & S_1 \end{Bmatrix}\begin{Bmatrix} L_{12} & L_{12} & 1 \\ L_2 & L_2 & L_1 \end{Bmatrix}\langle l_2^{N_2}\alpha_2 S_2 L_2 \| V^{(11)} \| l_2^{N_2}\alpha_2 S_2 L_2\rangle \Bigg] \\
&\quad+b^{11}_{n_3 l_3}\begin{Bmatrix} S & S & 1 \\ S_3 & S_3 & S_{12} \end{Bmatrix}\begin{Bmatrix} L & L & 1 \\ L_3 & L_3 & L_{12} \end{Bmatrix}\langle l_3^{N_3}\alpha_3 S_3 L_3 \| V^{(11)} \| l_3^{N_3}\alpha_3 S_3 L_3\rangle \Bigg]\Bigg]
\end{aligned}
$$

in which the radial integrals $b^{k_s k_l}_{n_i l_i}$ are analogous to the $a^{k_s k_l}_{n_i l_i}$ appearing in the dipole interaction. If these expressions are used to evaluate A or B values arising from only 1 or 2 partially filled shells, the quantum numbers and radial quantities for any unoccupied shells should be set equal to zero. References to sources giving tabulations of the required reduced matrix elements are given in Ref. 10.

Although these expressions are extremely general, they simplify considerably for any particular term. Thus for the $^{11}F_J$ term of $4f^7 5d^2 6s$ considered, the expressions for $A(J)$ and $B(J)$ reduce to

$$
\begin{aligned}
A(^{11}F_J)=\left[\frac{2J+1}{J(J+1)}\right]^{1/2}\Bigg[&(-1)^{J+1}\begin{Bmatrix} J & J & 1 \\ 3 & 3 & 5 \end{Bmatrix}2(3\times 7)^{1/2}a^{01}_{5d} \\
&+\begin{Bmatrix} 5 & 5 & 1 \\ 3 & 3 & 2 \\ J & J & 1 \end{Bmatrix}(2\times 3)[(3\times 11)/(5\times 7)]^{1/2}a^{12}_{5d} \\
&+(-1)^{J+1}\begin{Bmatrix} J & J & 1 \\ 5 & 5 & 3 \end{Bmatrix}[(2\times 11\times 3)/5)]^{1/2}A^{10}\Bigg]
\end{aligned}
$$

in which $A^{10}=\frac{1}{2}(7a^{10}_{4f}+2a^{10}_{5d}+a^{10}_{6s})$, and

$$B(^{11}F_J)=2\left[\frac{J(2J-1)(2J+1)}{(J+1)(2J+3)}\right]^{1/2}\left\{(-1)^J\begin{Bmatrix}3&3&2\\J&J&5\end{Bmatrix}2[3/(5\times7)]^{1/2}b^{02}_{5d}-\begin{Bmatrix}5&5&1\\3&3&3\\J&J&2\end{Bmatrix}\tfrac{3}{5}\left(\tfrac{11}{2}\right)^{1/2}b^{13}_{5d}+\begin{Bmatrix}5&5&1\\3&3&1\\J&J&2\end{Bmatrix}\tfrac{1}{5}(3\times7\times11)^{1/2}b^{11}_{5d}\right\}.$$

[1]The results of this work are summarized in *Atomic Energy Levels, the Rare Earth Elements,* Natl. Bur. Stand. Ref. Data Ser., Natl. Bur. Stand. (U.S.) Circ. No. 60, edited by W. C. Martin, R. Zalubas, and L. Hagen (U.S. GPO, Washington, D. C., 1978).

[2]References to much of this work can be found in G. H. Fuller, J. Phys. Chem. Ref. Data **5**, 835 (1976), and in Ref. 3.

[3]K. T. Cheng and W. J. Childs, Phys. Rev. A **31**, 2775 (1985).

[4]P. J. Unsworth, J. Phys. B (London) **2**, 122 (1969).

[5]M. D. Plimmer, P. E. G. Baird, D. N. Stacey, and G. K. Woodgate, Onzieme Conference Internationale de Physique Atomique, Paris, 1988, Resume VIII-20 (unpublished).

[6]G. Klemz and H. D. Kronfeldt, 20th EGAS Conference, Graz, Austria, July, 1988, Abstract A4-9 (unpublished).

[7]W. J. Childs and U. Nielsen, Phys. Rev. A **37**, 6 (1988).

[8]J. L. Hall and S. A. Lee, Appl. Phys. Lett. **24**, 367 (1976).

[9]*Tables of Spectral-Life Intensities, Arranged by Elements,* Natl. Bur. Stand. (U.S.) Monograph No. 145, edited by W. F. Meggers, C. H. Corliss, and B. F. Scribner (U. S. GPO, Washington, D. C., 1975).

[10]See, for example, W. J. Childs, Case Stud. At. Phys. **3**, 215 (1973).

[11]See, for example, B. G. Wybourne, *Spectroscopic Properties of Rare Earths* (Wiley, New York, 1965), p. 147.

[12]P. G. H. Sandars and J. Beck, Proc. R. Soc. London, Ser. A **289**, 97 (1965).

[13]This work is well summarized by S. Buttgenbach, *Hyperfine Structure in 4d-and 5d-Shell Atoms* (Springer-Verlag, Berlin, 1982).

[14]C. F. Fischer (private communication).

[15]W. J. Childs, Phys. Rev. A **2**, 316 (1970).